

Reliability Estimation for Power Factor Correction Circuits

Kumar A. Praveen¹ Amer Gulam² Rao.S Srinivasa³

Abstract-Reliability plays an important role in power electronic systems such as spacecrafts, aircrafts and telecommunications. Therefore it is necessary to calculate the failure rate, repair cost etc before designing a power supply for such applications. In this paper single switch boost Power Factor Correction (PFC) converter and interleaved boost PFC converter is simulated in Discontinuous Conduction Mode (DCM), Critical Conduction Mode (CRM) and Continuous Conduction Mode (CCM) under different output power ratings and results are tabulated. The reliability of semiconductor devices and all other components of the converter are calculated based on MIL-HDBK-217 standard. From the simulation results it is found that both single switch boost PFC converter and interleaved boost PFC converter performance when operating in CCM is better with reference to reliability.

Keywords - Reliability, Power factor correction, Boost Converter, Simulation of converters.

I. INTRODUCTION

Reliability is the probability of operating a product for a given period of time without failure under specified conditions and within specified performance limits. It plays an important role in power electronic systems by which the number of system failures, repair costs, guarantee etc are estimated. Every day the dependency upon the continuous availability of electronic equipment grows [1]. Examples include telephone systems, computers supporting stock markets, and industrial control equipment, petrochemicals etc. This means the power supplies supporting the equipments/loads must perform without interruption and without any fault. The design emphasis in power-electronic systems is primarily on (apart from production cost) efficiency, power density and quality; the assumption being, if these criteria are met then, once a power-electronic product or system is in service, it will last for a long time (i.e. it have a high mean time to failure or MTTF). This is not a rational expectation and as such, many of the power-supply and power-system industries are faced with the daunting reality of random product and system failures in the field at a steady rate, which is costing the industries a lot. Many power-supply/power-system industries have expressed the need for investigating failure modes of their products/systems to significantly increase the MTTF and the mean time between failures (MTBFs). However, this is not an easy task which requires an extensive multidisciplinary effort.

The paper first received 5-Jun-2009 and in revised form 16-Sept- 2009.
Digital Ref: A17050229

¹ Department of Electrical Engineering, National Institute of Technology

² Department of Electrical Engineering, National Institute of Technology Warangal, Andhra Pradesh, India E-mail: amer.nitw@gmail.com

³ Department of Electrical Engineering, National Institute of Technology Warangal, Andhra Pradesh, E-mail: srinivasarao_nitw@yahoo.co.in

A. Reliability Function

The reliability of a component can be described as an exponential function [1]. The probability of finding a component operating after a time period is defined as:

$$R(t) = e^{-\lambda t} \quad (1)$$

Where λ is the constant failure rate during the useful life period. The mathematic mean value of $R(t)$ occurs at t equal to $1/\lambda$. It is the mean time elapsed until a failure which occurs, or the "Mean Time To Failure", MTTF. Reliability curve is shown in Fig. 1.

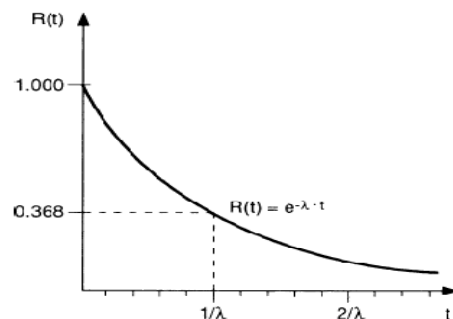


Fig.1 Reliability curve [1]

MTBF (Mean Time between Failures): As repair time (MTTR) normally can be neglected compared to MTTF for electronics, MTBF can be found as :

$$\begin{aligned} \text{MTBF} &= \text{MTTF} + \text{MTTR} \\ &\approx \text{MTTF} = 1/\lambda \end{aligned}$$

MTBF or the failure rate can be calculated using different kinds of input data.

B. Time Dependence of Failure Rate

The time dependence of the failure rate for a given population of items of the same type often exhibits at least one of the following three periods which produce a bathtub curve as in Fig. 2.

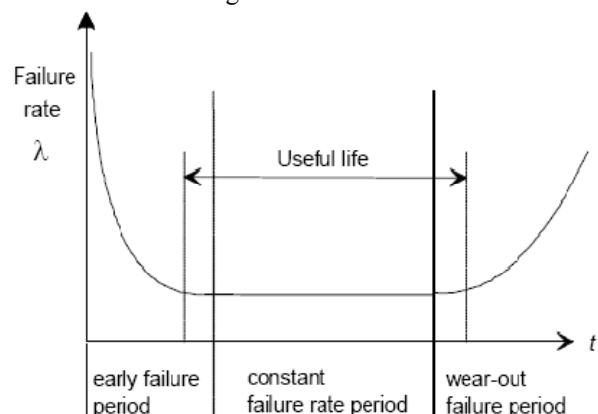


Fig. 2 Time dependence of the failure rate

When interpreting reliability figures it is important to determine the physical reality of failure modes and distributions. These three periods can be explained as in the following. However, the time dependence curve for any single item type could be significantly different.

1. *Early failure period*: At the start of the operating period, sometimes a higher failure rate is observed which decreases with time. Early failures occur due to manufacturing processes and material weaknesses that do not result in failures in tests.
2. *Constant failure rate period*: After the early failure period, the failures occur with varying failure causes that result in an effective constant failure rate during the useful life.
3. *Wear-out failure period*: The final period that shows an increasing rate of failures due to the dominating effects of wear-out, ageing or fatigue.

C. Calculation of MTBF for Equipment

When calculating the MTBF for equipment [1], its total failure rate λ_e must be found. Normally the assumption is that all components are needed for operation. Consider an equipment or apparatus containing n components. The probability to find n components in operation after the time t is:

$$R = R_1 \cdot R_2 \cdot \dots \cdot R_n = e^{-\lambda_1 t} \cdot e^{-\lambda_2 t} \cdot \dots \cdot e^{-\lambda_n t} = e^{-(\lambda_1 + \lambda_2 + \dots + \lambda_n)t} = e^{-\lambda_e t} \quad (2)$$

and

$$\lambda = \lambda_1 + \lambda_2 + \lambda_3 + \dots + \lambda_n \quad (3)$$

The total failure rate for the equipment at specified conditions is accordingly achieved as:

$$\lambda_e = \lambda_{b1} \cdot c_1 + \lambda_{b2} \cdot c_2 + \dots + \lambda_{bn} \cdot c_n \quad (4)$$

By simply inverting this value, the MTBF figure for the equipment is found:

$$MTBF = \frac{1}{\lambda_e} \quad (5)$$

D. Reliability Prediction [2]

Reliability predictions are conducted during the concept and definition phase, the design and development phase and the operation and maintenance phase, at various system levels and degrees of detail, in order to evaluate, determine and improve the dependability measures of an item. Successful reliability prediction generally requires developing a reliability model of the system considering its structure. The level of detail of the model will depend on the level of design detail available at the time. Several prediction methods are available depending on the problem. During the conceptual and early design phase a failure rate prediction is a method that is applicable mostly, to estimate equipment and system failure rate. Following models for predicting the failure rate of items are given:

- failure rate prediction at reference conditions (parts count method)
- failure rate prediction at operating conditions (parts stress method)

Failure rate predictions are useful for several important activities in the design phase of electronic equipment in

addition to many other important procedures to ensure reliability. Examples of these activities are:

- to assess whether reliability goals can be reached,
- to identify potential design weaknesses,
- to compare alternative designs,
- to evaluate designs and to analyze life-cycle costs,
- to provide data for system reliability and availability analysis,
- to plan logistic support strategies,
- to establish objectives for reliability tests.

E. Parts Count Method

In this paper, parts count method is used. The failure rate for equipment under reference conditions is calculated as follows:

$$\lambda_{s,t} = \sum_{i=1}^n (\lambda_{ref})_i \quad (6)$$

where

λ_{ref} is the failure rate under reference conditions
 n is the number of components

The reference conditions adopted are typical for the majority of applications of components in equipment. Reference conditions include statements about operating phase, failure criterion, operation mode (e.g. continuous, intermittent), climatic, mechanical stresses and electrical stresses. It is assumed that the failure rate used under reference conditions is specific to the component, i.e. it includes the effects of complexity, technology of the casing, different manufacturers and the manufacturing process.

F. Parts Stress Method

Components in equipment may not always operate under the reference conditions. In such cases, the real operational conditions will result in failure rates different from those given for reference conditions. Therefore, models for stress factors, by which failure rates under reference conditions can be converted to values applying for operating conditions (actual ambient temperature and actual electrical stress on the components), and vice versa, may be required. The failure rate for equipment under operating conditions is calculated as follows:

$$\lambda = \sum_{i=1}^n (\lambda_{ref} \times \pi_U \times \pi_I \times \pi_T)_i \quad (7)$$

where

λ_{ref} is the failure rate under reference conditions;
 π_U is the voltage dependence factor;
 π_I is the current dependence factor;
 π_T is the temperature dependence factor;
 n is the number of components

II. SINGLE SWITCH BOOST PFC RECTIFIER

The operation of boost PFC converter can be studied under three modes of operations viz. continuous conduction mode, discontinuous conduction mode and critical conduction mode. The continuous conduction mode is studied and simulated for three current control modes-

peak current mode control, average current mode control and hysteresis current mode control. Fig. 3 shows the schematic diagram of boost PFC converter.

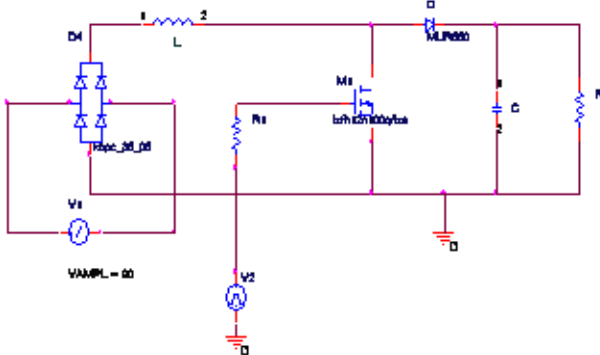


Fig. 3 Boost PFC rectifier

A. Continuous Conduction Mode of Operation

The operation of boost PFC converter for Continuous conduction mode is studied and simulated under voltage control mode and current control mode. The current control mode is simulated under three modes namely peak current mode control, average current mode control and hysteresis current control mode. By calculating the reliability under these three current control modes we can understand which method is best from the reliability point of view and also we can verify whether any of the three current control modes is inferior in reliability to DCM and CRM modes.

(a) Peak Current Mode Control:

The current control signal i^* which is a scaled input voltage determines the peak of the inductor current i_L , the sinusoidal current reference. This reference is usually obtained by multiplying a scaled replica of the rectified line voltage v_g times the output of the voltage error amplifier, which sets the current reference amplitude. The active switch in the boost converter is turned on at the beginning of each switching cycle. The switch is turned on at constant frequency by a clock signal. As soon as the inductor current i_L reaches i^* , the switch is turned off and this process repeats [3]. In this way, the reference signal is naturally synchronized and always proportional to the line voltage, which is the condition to obtain unity power factor.

(b) Average Current Mode Control:

The inductor current is sensed and filtered by a current error amplifier whose output drives a PWM modulator. In this way the inner current loop tends to minimize the error between the average input current i_g and its reference. The latter is obtained in the same way as in the peak current control. Its advantage over the peak current mode control is that the stability ramp, which is mandatory for the peak current mode control, is eliminated. The inductor current waveform shown in fig 4.

(c) Hysteresis Current Mode Control:

The upper inductor current reference is a half sinusoidal denoted $I_p \sin \omega t$, with peak amplitude of I_p . The lower current reference is a half sinusoid, denoted $I_c \sin \omega t$, with peak amplitude of I_c . The average inductor current, which has only the 120 Hz component of inductor current, is a half sinusoid, denoted $I_m \sin \omega t$. The inductor current ripple is $\delta \sin \omega t$, where δ is the peak current ripple. Since the

inductor current switches at a much higher rate than the line voltage, the line voltage is assumed constant in each inductor current switching cycle [4] for the above current control mode techniques.

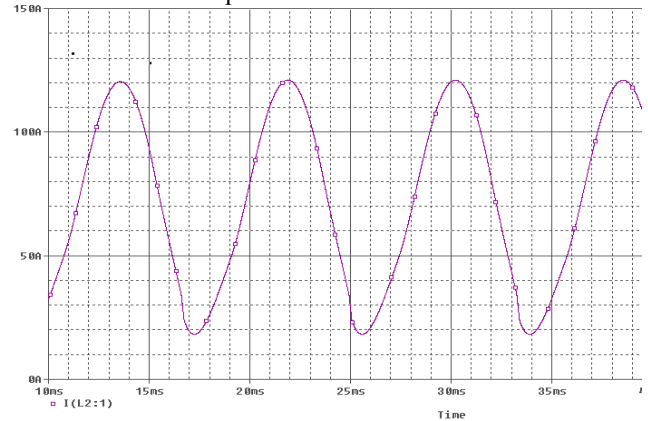


Fig. 4 Inductor current waveform for CCM- Average CMC

B. Discontinuous Mode of Operation

For low power application, to reduce the added component count and cost of the PFC stage in the two-stage approach, low cost alternatives have been rigorously pursued by attempting to integrate the active PFC input stage with the isolated DC/DC converter. The input PFC function is automatically achieved based on the principle of circuit operation. Generally, the input power factor of discontinuous PFC converter is not unity, but its input current harmonics are small enough to meet the specifications, such as the IEC 61000-3-2 class D [5]. The discontinuous conduction mode of boost PFC is simulated and the inductor current waveforms are shown in Fig.5 and Fig. 6.

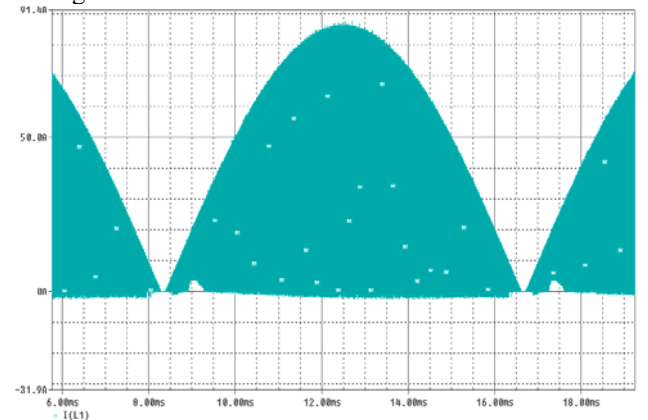


Fig. 5 Inductor current waveform for DCM

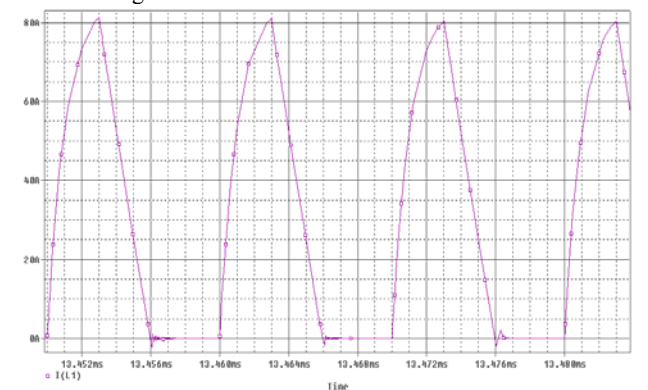


Fig.6 Inductor current for DCM (enlarged)

C. Critical Boost PFC Rectifier

The operation at the boundary of CCM and DCM was considered "constant on-time" for the boost switch. However, due to finite switching frequency and capacitor filter effect, the switch turn-on time varies throughout the entire cycle. This variation of the switch "on-time" affects the average switching frequency and the circuit component selection criterion. The control switch turns on when the inductor drops to zero and turns off when the inductor current reaches the peak inductor current envelope. The actual inductor current presents a saw tooth-type wave shape [6]. The simulated waveforms under critical conduction mode are shown in Fig. 7 and Fig. 8.

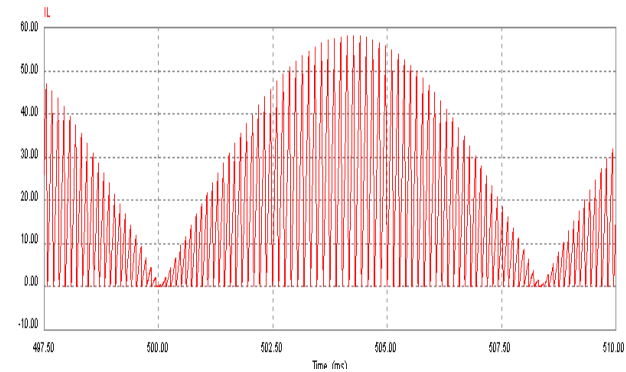


Fig.7 Inductor current waveform for CRM

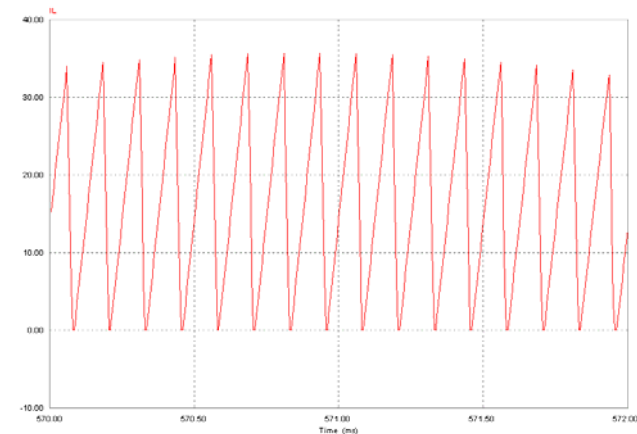


Fig.8 Inductor current waveform for CRM (enlarged)

III. INTERLEAVED BOOST PFC

Interleaved converters offer several advantages over single-power stage converters; a lower current ripple on the input and output capacitors, faster transient response to load changes and improved power handling capabilities at greater than 90% power efficiency. Another important advantage of interleaving is that it effectively increases the switching frequency without increasing the switching losses. The obvious benefit is an increase in the power density without the penalty of reduced power-conversion efficiency. There is still a penalty, however. Interleaving requires increased circuit complexity (greater number of power-handling components and more auxiliary circuitry), leading to higher parts and assembly cost and reduced reliability. Fig.9 shows the schematic diagram of interleaved Boost PFC [7-8].

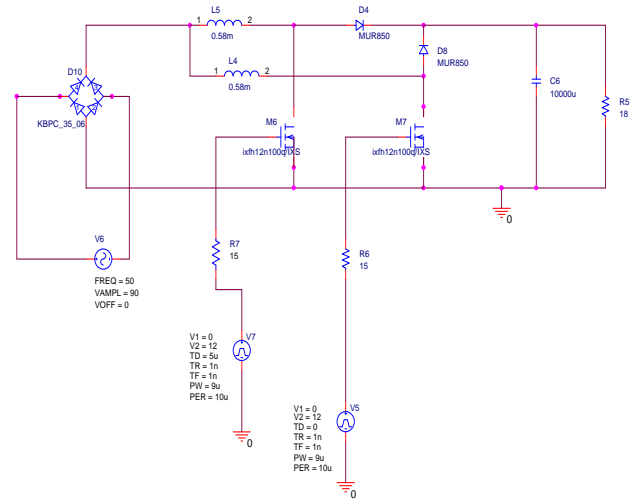


Fig. 9 Interleaved Boost Converter Topology

A. Continuous Conduction Mode

Even though the inductor currents in I_{L1} and I_{L2} are discontinuous the input current which is the sum of two inductor currents is continuous [9]. So that interleaving virtually eliminates discontinuity in the input current which is a major advantage. The inductor current waveform for continuous conduction mode of interleaved converter is shown in Fig. 10

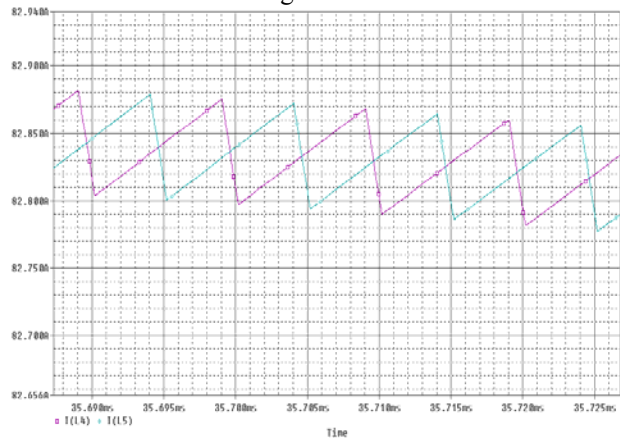


Fig. 10 Inductor current waveforms for Interleaved CCM (enlarged)

B. Discontinuous Mode of operation

To operate interleaving configuration in discontinuous mode of operation the phase shift of 180° is properly incorporated between the two inductor currents by using the delay. Fig. 11 shows the boost inductor current waveforms in discontinuous mode of operation.

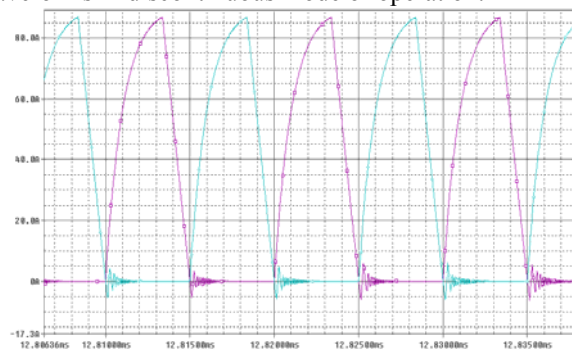


Fig. 11 Inductor currents waveforms (enlarged) for interleaved DCM boost

C. Critical Conduction Mode

The interleaved switching converter composed of parallel connection of switching converters of the same switching frequency, but each switching phase is sequentially shifted over equal fractions of the switching period [10]. The simulated CRM inductor current waveforms have been shown in Fig.12.

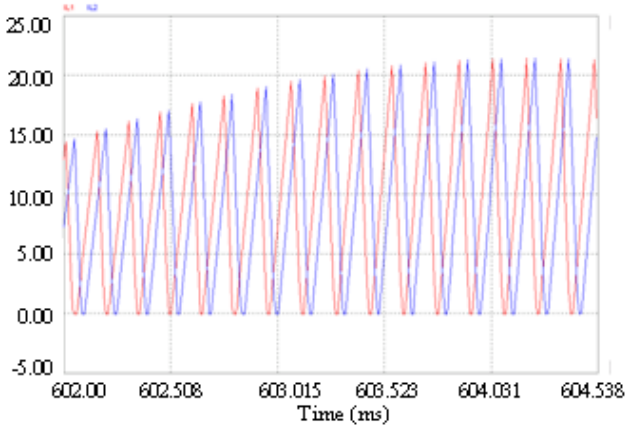


Fig. 12 Inductor currents for Interleaved CRM (enlarged)

IV. RELIABILITY CALCULATIONS [11]

In this section, reliability of the boost converter in 1200 W output power and Peak Current Mode control is calculated and presented in details. For different output powers and operating modes, results of reliability calculations are shown in Table-IV to Table-VI. The parts count method is used to calculate reliability. In this approach, first the failure rate of each component in the converter configuration is obtained individually and then the value of the converter’s MTBF is calculated from equations (4) and (5) that “N” is the number of consisting parts. The reliability of semiconductor devices and all other components of the converter are calculated based on MIL-HDBK-217 standard [12]. MIL-HDBK-217 provides failure rate data and stress models for parts count and parts stress predictions. It provides models for many component and assembly types and fourteen environments ranging from ground benign to canon launch. It is well known for international military and commercial design procedures has been widely accepted. It provides predictions for ambient of 0°C to 125°C. For these calculations the following assumptions are made:

1. The ambient temperature is 27 °C
2. The control structures of these converters are not the same whose reliability can be neglected for comparing the reliability of main components.
3. To calculate the reliability, first the dynamic and static losses of MOSFET and diode should be calculated for different output powers working in three operating modes namely CCM, DCM and CRM.

$$P_{dynamic} = V_{avg} \times I_{avg} \times t_{ol} \times f_s \tag{8}$$

$$P_{static} = V_{on} \times I_{avg} \times t_{on} \times f_s \tag{9}$$

$$P_{loss} = P_{static} + P_{switching} \tag{10}$$

It should be noted that if the converter is operating in DCM mode, ensure that before further turn-on of the switch, the inductor current reaches to zero. So that there will not be turn-on loss. But in CCM operating mode, since in turn-on instant for the switch, the current should

be transferred from diode to the switch, the dynamic loss includes both turn-on/turn-off losses. Sample simulated diagrams for MOSFET and diode switching wave forms have been shown in Fig. 12 – 16.

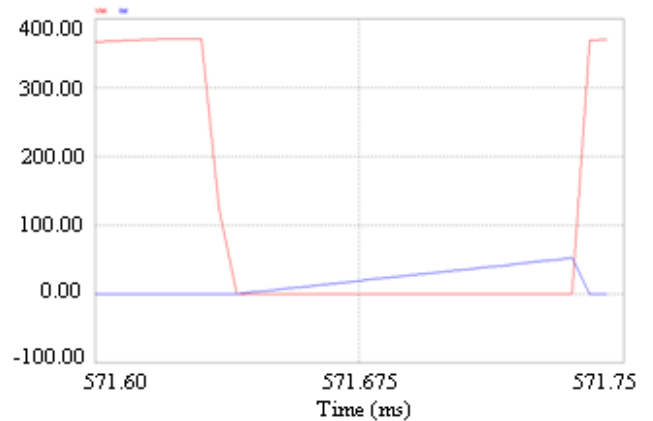


Fig. 13 MOSFET switching waveform for 1200W- CRM.

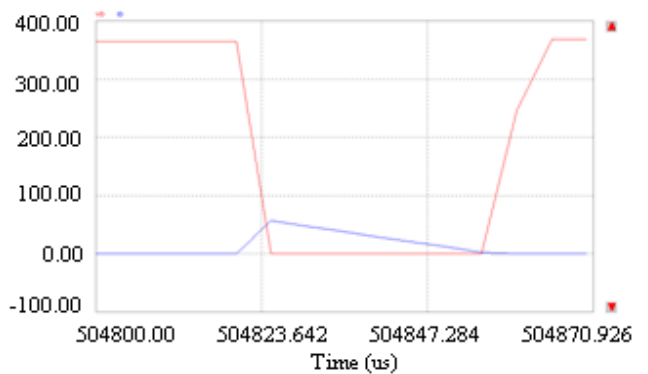


Fig. 14 Diode switching waveform for 1200W- CRM.

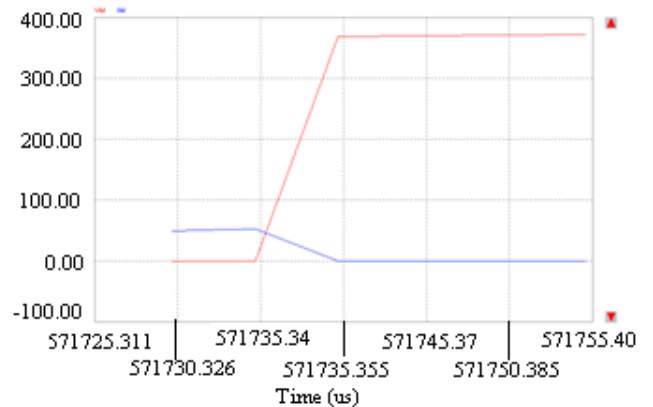


Fig. 15 Turn-off overlap of MOSFET waveform for 1200W- CRM

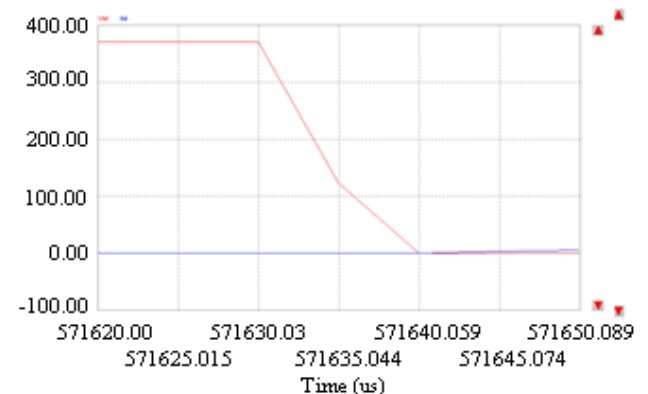


Fig. 16 Turn-on overlap of MOSFET waveform for 1200W- CRM

V. RESULTS AND CONCLUSIONS

A. Discussion of Result

The power loss is calculated for each component in the converters under specified operating modes and tabulated in Tables I, II and III. Then, the reliability is calculated and compared for CCM (namely Peak-CMC, Average-CMC and Hysteresis-CMC), DCM and CRM for the converters and tabulated in tables IV, V and VI.

B. Conclusions

From Table IV, V, VI the following points are observed.

- The Boost Converter has highest reliability in CCM operating mode than in DCM and CRM.

- Switches have highest failure rate in DCM and CRM modes than CCM mode. Since in DCM and CRM modes the peak and rms values of current are higher that results in higher current stress on switches in this mode. Therefore failure rate is higher in CRM and then DCM compared to CCM.
- The results concluded for single switch boost PFC are true for interleaving configuration also. But the reliability of interleaved topology is much lesser compared to the single switch boost PFC because of the presence of two inductors, two diodes and two MOSFETs.

Table-1: Calculated power loss for each component of the boost PFC rectifier

Output Power	800W			1000W			1200W		
	Peak	Average	Hysteresis	Peak	Average	Hysteresis	Peak	Average	Hysteresis
P _{dynamic} (MOSFET)	27.032292	49.614022	93.5101	28.7910	42.62004	73.416	33.787	40.68318	50.4336
P _{static} (MOSFET)	27.34746	43.9747	100.0123	27.81144	39.2316	78.46335	35.376875	43.3254	52.53623
P _{dynamic} (DIODE)	0.94956	1.2294	1.819272	1.270665	2.4239	3.889664	1.9836	1.9986	5.472
P _{static} (DIODE)	0.017835	0.0266568	0.051156	0.029445	0.030247	0.2752386	0.006961	0.00232	0.01152
Input Bridge	3.70128	3.7224	3.79104	3.84384	3.85176	3.86496	3.8808	3.91776	3.96

Table-II Calculated power loss for boost PFC under DCM and CRM

Output Power	800W		1000W		1200W	
	DCM	CRM	DCM	CRM	DCM	CRM
P _{dynamic} (MOSFET)	258.44364	251.4707	229.7106	235.36	135.6885	152.9867
P _{static} (MOSFET)	0.1027628	22.2179	0.094374	26.668	0.02777	23.8866
P _{dynamic} (DIODE)	41.90355	128.1775	30.9852	141.3348	19.1568	166.6692
P _{static} (DIODE)	0.005655	0.16228	0.038627	0.108703	0.0054375	0.30942
Input Bridge	4.32432	5.16912	4.752	5.3724	5.7024	6.115824

Table-III Calculated power losses for MOSFET, output diode and the input bridge for interleaved boost converter

Output Power	800W			1000W			1200W		
	CCM	DCM	CRM	CCM	DCM	CRM	CCM	DCM	CRM
$P_{dynamic}$ (MOSFET) Watts	71.4604	235.4625	238.05197	106.657	23.5172	318.1074	119.238	425.044125	451.6391
P_{static} (MOSFET) Watts	40.85928	0.1029	0.03659	19.36	5.4931	0.169814	17.768	0.25276	0.326604
$P_{dynamic}$ (Output Diode) Watts	2.2758	60.732	76.650435	11.4468	12.2972	52.02252	2.5245	52.24275	56.25371
P_{static} (Output Diode) Watts	0.036125	0.005156	0.0019575	0.162	0.0971	0.018125	0.03912	0.0098	0.04902
P_{loss} (Input Bridge) Watts	2.5476	4.32432	4.7256	2.75616	4.9896	5.2008	2.86704	5.89248	6.0984

Table-IV Reliability calculations for CCM operating mode for single switch boost PFC

Output Power	800W			1000W			1200W		
	Peak	Average	Hysterisis	Peak	Average	Hysterisis	Peak	Average	Hysterisis
λ_p (MOSFET)	15.38	29.64	88.85	16.04	24.81	60.52	20.12	25.66	33.85
λ_p (Output Diode)	0.363	0.412	0.453	0.065	0.073	0.087	0.041	0.05	0.06
λ_p (Input Bridge)	0.241	0.250	0.2656	0.143	0.155	0.164	0.104	0.110	0.113
λ_p (Input Inductor)	0.251	0.251	0.233	0.251	0.251	0.233	0.251	0.251	0.233
λ_p (Output Capacitor)	0.060	0.06	0.06	0.07	0.07	0.07	0.084	0.084	0.084
λ_p (Output Resistor)	0.03	0.03	0.03	0.03	0.03	0.03	0.03	0.03	0.03
Total λ_p	16.32	30.64	89.89	16.60	25.39	61.10	20.63	26.18	34.37
MTBF (hours)	61267	32631	11124	60234	39389	16365	4846	38194	29093

Table-V Reliability calculations for DCM and CRM operating modes of single switch boost PFC

Output Power	800W		1000W		1200W	
	DCM	CRM	DCM	CRM	DCM	CRM
λ_p (MOSFET)	141.25	154.56	117.04	144.28	50.86	76.96
λ_p (Output Diode)	3.90	20.12	0.66	9.72	0.075	4.10
λ_p (Input Bridge)	0.18	0.21	0.19	0.20	0.16	0.17
λ_p (Input Inductor)	0.18	0.18	0.18	0.18	0.18	0.18
λ_p (Output Capacitor)	0.06	0.06	0.07	0.07	0.084	0.084
λ_p (Output Resistor)	0.03	0.03	0.03	0.03	0.03	0.03
Total λ_p	145.60	175.17	118.16	154.48	51.391	81.54
MTBF (hours)	6868	5708	8463	6473	19458	12264

Table-VI Reliability calculations for CCM, DCM and CRM operating modes of interleaving boost PFC

Output Power	800W			1000W			1200W		
	CCM	DCM	CRM	CCM	DCM	CRM	CCM	DCM	CRM
λ_p (MOSFET)	76.686	256.9	261.11	90.92	390.41	391.16	103.20	601.56	655.33
λ_p (Output Diode)	0.200	2.030	3.145	0.58106	2.776	3.1293	0.60	5.014	5.86
λ_p (Input Bridge)	0.103	0.124	0.139	0.14213	0.169	0.181	0.173	0.209	0.222
λ_p (Input Inductor)	0.509	0.363	0.362	0.5099	0.362	0.362	0.5099	0.362	0.362
λ_p (Output Capacitor)	0.060	0.060	0.060	0.0713	0.071	0.071	0.084	0.084	0.084
λ_p (Output Resistor)	0.0297	0.0297	0.0297	0.0297	0.0297	0.0297	0.0297	0.0297	0.0297
Total λ_p	77.59	259.46	264.85	92.25	93.82	394.94	104.60	607.26	661.19
MTBF (hours)	12888	3854	3775	10839	10658	2532	9560	1646	1512

ACKNOWLEDGMENT

We thank the Department of Electrical Engineering, National Institute of Technology, Warangal for providing excellent environment to do this work.

APPENDIX

In this section, the sample calculation for failure rate for each component is presented:

a) Calculation of Failure rate λ_p for MOSFET (IXFH12N100Q/IXS) :

$$V_n=1000V, \theta_{jc}=0.42^\circ C/W, \theta_{ca}=1^\circ C/W$$

$$T_c = T_a + \theta_{ca} \times P_{loss} = 27+1 \times 69.163875=96.163875$$

$$T_j = T_c + \theta_{jc} \times P_{loss} = 96.163875+0.42 \times 69.163875 = 125.2127$$

$$\pi_T = \exp\left(-1925 \times \left(\frac{1}{T_j+273} - \frac{1}{298}\right)\right) = 5.08162$$

$$\lambda_b=0.012, \pi_E=6, \pi_A=10, \pi_Q=5.5$$

$$\lambda_p = \lambda_b \times \pi_Q \times \pi_E \times \pi_A \times \pi_T = 0.012 \times 5.5 \times 6 \times 10 \times 5.08162 = 20.1232$$

b) Calculation of failure rate (λ_p) for Output diode:

$$V_n=1000V, \theta_{jc}=2^\circ C/W, \theta_{ca}=1, P_{loss}=1.99056W$$

$$T_c = T_a + \theta_{ca} \times P_{loss} = 27+1 \times 1.99056 = 28.99056$$

$$T_j = T_c + \theta_{jc} \times P_{loss} = 27+ 1 \times 1.99056 = 32.97168$$

$$\pi_T = \exp\left(-1925 \times \left(\frac{1}{T_j+273} - \frac{1}{298}\right)\right) = 1.183291$$

$$\lambda_b=0.069, \pi_E=6, \pi_Q=5.5, \pi_C=1$$

$$V_S = \frac{90}{500} = 0.18 \Rightarrow \pi_S = V_S^{2.43} = 0.01549$$

$$\lambda_p = \lambda_b \times \pi_Q \times \pi_S \times \pi_E \times \pi_T \times \pi_C = 0.069 \times 5.5 \times 0.015 \times 6 \times 1.183291 \times 1 = 0.041735$$

c) Calculation of failure rate(λ_p) for Input Bridge:

$$V_n=1000V, \theta_{jc}=1.6^\circ C/W, P_{loss}=3.8808 W$$

$$T_c = T_a + \theta_{ca} \times P_{loss} = 27+ 1 \times 3.8808 = 30.8808$$

$$T_j = T_c + \theta_{jc} \times P_{loss} = 30.8808 + 1.6 \times 3.8808 = 37.09008$$

$$\pi_T = \exp\left(-1925 \times \left(\frac{1}{T_j+273} - \frac{1}{298}\right)\right) = 1.286413$$

$$\lambda_b=0.069, \pi_E=6, \pi_Q=5.5, \pi_C=1$$

$$V_S = \frac{304}{1200} = 0.2533 \Rightarrow \pi_S = V_S^{2.43} = 0.03554$$

$$\lambda_p = \lambda_b \times \pi_Q \times \pi_E \times \pi_C \times \pi_S \times \pi_T = 0.069 \times 5.5 \times 6 \times 1 \times 0.03554 \times 1.286413 = 0.104102$$

d) Calculation of failure rate(λ_p) for Inductor:

$$T_{HS} = T_A + 1.1 \times \Delta T = 27 + 1.1 \times 11 = 39.1$$

$$\lambda_b = 0.0016 \times \left(\frac{T_{HS} + 273}{329}\right)^{15.6} = 0.70282m$$

$$\pi_E=6, \pi_Q=20;$$

$$\lambda_p = \lambda_b \times \pi_Q \times \pi_E = 0.070282 \times 10^{-3} \times 6 \times 20 = 0.08433$$

e) Calculation of failure rate for Capacitor:

$$\Pi_{CV} = 0.34 \times C^{0.18} = 0.34 \times (917\mu)^{0.18} = 0.09653$$

$$\pi_E=2, \pi_Q=10;$$

$$\lambda_p = \lambda_b \times \pi_Q \times \pi_E \times \pi_{CV} = 0.13 \times 10 \times 2 \times 0.09653 = 0.250978$$

f) Calculation of failure rate for Resistor:

$$\pi_R=1, \pi_E=2, \pi_Q=10, \lambda_b = 0.000066;$$

$$\lambda_p = \lambda_b \times \pi_Q \times \pi_E \times \pi_R = 0.00066 \times 10 \times 2 \times 1 = 0.0297$$

Therefore the total system failure rate will be:

$$\lambda_{system} = \sum_{n=1}^N \lambda_{part} = 20.634 \text{ (failures/ } 10^6 \text{ hours)}$$

$$\Rightarrow MTBF = \frac{1}{\lambda} = 48463.70$$

REFERENCES

- [1] Reliability aspects on power supplies, design note 02 EN/LZT 14600 RIA (C Ericsson Microelectronics AB, April, 2001).
- [2] European power supply manufacturing association, "Guidelines for understanding Reliability Prediction", June, 2005
- [3] C. Zhou, M. Jovanovic, "Design trade-offs in continuous current-mode controlled boost power-factor correction circuits", HFPC Conf. proc. May 1992, pp. 209-219.
- [4] C. Zhou, R. B. Ridley and F. C. Lee, "Design and analysis of a hysteretic boost power factor correction circuit", PESC Conf. Proc.1990, pp. 800-807.
- [5] Jindong Zhang, "Advanced integrated single stage power factor correction techniques" Ph.D thesis, Virginia tech., 15 March 2001.
- [6] Dao-Shen Chen, Jih-Sheng Lai, "A Study of power correction boost converter operating at CCM-DCM mode", Proceedings of IEEE Southeastcon'93, 4-7 Apr 1993.
- [7] Chin Chang; Knights, M.A. "Interleaving technique in distributed power conversion systems", IEEE Transactions on Circuits and Systems: Fundamental Theory and Applications, Vol. 42, Issue 5, May 1995, pp.245 – 251.
- [8] Takuya Ishii and Yoshio Mizutani, "Power Factor Correction using Interleaving Technique for Critical Mode Switching Converters", PESC'98, Vol.1, May 1998, pp. 905-910.
- [9] B.A. Miwa and M.F. Schlecht, "High efficiency power factor correction using interleaving techniques", Applied Power Electronics Conference and Exposition (APEC '92), 23-27 Feb. 1992, pp.557 - 568.

- [10] Abdi, M.B.Menhaj, L.Yazdanparast, J.Milimonfared, "The effect of the transformer winding on the reliability of switching power supplies", 12th International PEMC Aug 2006- Sept 2006, pp.663 – 667.
- [11] B.Abdi, A.H.Ranjbar, J.Milimonfared, .B.Gharehpetian, "Reliability comparison of boost PFC converter in DCM and CCM operating modes", International Symposium on Power Electronics, Electrical Drives, Automation and Motion Conference (SPEEDAM), 11-13 June 2008, pp: 939-943.
- [12] MIL-HDBK-217, "Reliability prediction of electronic equipment", 1991.

BIOGRAPHIES



A. Praveenkumar received his B. Tech degree in electrical engineering from Jawaharlal Nehru Technological University, Anantapur, India in 2006. and M. Tech degree from National Institute of Technology, Warangal India in 2009. His research interests include DC-DC converter for power factor correction, Distributed power system.



Gulam Amer has obtained the B.E. in instrumentation engineering from Osmania University, Hyderabad, India in 2002 and M.Tech in Power Electronics from Vishweshwaraya technological university, Belgaum, India. He is presently doing research at National Institute of Technology Warangal, India.. His research interests include DC-DC Converter, SMPS, Power factor correction circuits, distributed power system and telecom power supply. He is the life member of ISTE and BMESI. He is also student member of IEEE.



S. Srinivasa Rao received his B.Tech degree in electrical engineering from Regional Engineering College, Warangal, India, in 1992 and M. Tech degree from Regional Engineering College, Calicut, India, in 1994. He obtained his Ph. d degree from National Institute of Technology Warangal in 2007. Since 1996 he is working as a faculty member in National Institute of Technology Warangal, India. He published many papers in international journals and conferences. His research interests include power electronic drives, DSP controlled drives and non-conventional power generation. He is a Life Member in Systems Society of India (SSI) and Society for Technical Education (ISTE) and Member in Institution of Engineers (India).